Published in final edited form as:
Hepatol Res. 2012 November ; 42(11): 1119–1130. doi:10.1111/j.1872-034X.2012.01026.x.

Novel Organotypic Culture Model of Cholangiocarcinoma Progression

Deanna J. W. Campbell[1], **Catherine I. Dumur**[1], **Nadia F. Lamour**[1], **Jennifer L. DeWitt**, and **Alphonse E. Sirica**
Department of Pathology, Division of Cellular and Molecular Pathogenesis, Virginia Commonwealth University School of Medicine, Medical College of Virginia Campus, Richmond, Virginia 23298-0297

Abstract

Aims—Recent studies have suggested that increased α-smooth muscle-actin-positive myofibroblastic cells (α-SMA-positive CAFs) in the desmoplastic stroma may relate to a more aggressive cancer and worse survival outcomes for intrahepatic cholangiocarcinoma (ICC) patients. To facilitate investigating cellular and molecular interactions between α-SMA-positive CAFs and cholangiocarcinoma cells related to ICC progression, we developed a novel 3-dimensional (3-D) organotypic culture model of cholangiocarcinoma that more accurately mimics the stromal microenvironment, gene expression profile, and select pathophysiological characteristics of desmoplastic ICC *in vivo*.

Methods—This unique model was established by co-culturing within a type I collagen gel matrix, a strain of cholangiocarcinoma cells (derived from an ICC formed in syngeneic rat liver following bile duct inoculation of spontaneously-transformed rat cholangiocytes) with varying numbers of clonal α-SMA-positive CAFs established from the same tumor type.

Results—Cholangiocarcinoma cells and α-SMA-positive CAFs in monoculture each exhibited cell specific biomarker gene expression profiles characteristic of stromal myofibroblastic cell *versus* malignant cholangiocyte cell types. In comparison, the gene expression profile and histopathological characteristics exhibited by the organotypic co-culture closely resembled those of whole tissue samples of the parent orthotopic ICC. We further showed α-SMA-positive CAFs to significantly enhance cholangiocarcinoma cell “ductal-like” growth and cancer cell migration/invasiveness *in vitro*, as well as to promote up-regulated expression of select genes known to be associated with ICC invasion.

Conclusions—This novel organotypic model provides an important new resource for studying the effects of microenvironment on cholangiocarcinoma progression *in vitro* and may have potential as a preclinical model for identifying molecularly targeted therapies.

Introduction

Cancer-associated fibroblastic cells (CAFs) immunoreactive for α-smooth muscle actin (α-SMA) are a major cellular component of the desmoplastic stroma of primary cholangiocarcinomas formed in liver (1–3). Although largely descriptive, there is

Corresponding Author: Dr. Alphonse E. Sirica, Department of Pathology, Division of Cellular and Molecular Pathogenesis, Virginia Commonwealth University School of Medicine, P.O. Box 980297, Richmond, Virginia 23298-0297. Telephone No.: (804) 828-9549; Fax No.: (804) 828-4077; asirica@mcvh-vcu.edu.
[1]DC, CD, and NL contributed equally to the data generated in this study.

Conflicts of Interest: None

accumulating evidence to suggest that these myofibroblastic-like cells may have a crucial role in accelerating intrahepatic cholangiocarcinoma (ICC) progression (4, 5).

In humans, increased α-SMA-positive CAFs in the stroma of ICCs has been shown to correlate with larger tumor size and/or shorter patient survival times when compared with ICCs low in positive α-SMA stromal cell immunoreactivity (6, 7). Moreover, non-contact co-culturing of human cholangiocarcinoma cell lines (HuCCT1 or MEC) with either the immortalized myofibroblastic cell line LX-2 derived from human hepatic stellate cells (8) or the LI90 myofibroblastic cell line derived from a human hepatic mesenchymal tumor (9) was shown to significantly enhance cholangiocarcinoma cell proliferation and migration (invasion) *in vitro* over that exhibited by cholangiocarcinoma cells assayed in the absence of LX-2 or LI90 cells (6). Conditioned medium (CM) from LI90 cell cultures also significantly increased human HuCCT1 and RBE cholangiocarcinoma cell proliferation and invasion *in vitro* (10). Of further interest, CM from primary culture α-SMA-positive CAFs derived from a human cholangiocarcinoma was demonstrated in 2-dimensional (2-D) culture to stimulate a significantly greater cell proliferative response in cultured human KKU cholangiocarcinoma cell lines of varying states of differentiation, as well as in non-tumorigenic SV-40 immortalized human H-69 cholangiocytes, than that elicited by CM from primary cultures of normal skin fibroblasts or primary fibroblasts from non-tumorigenic liver (7).

While the results of the cell culture studies described above are clearly suggestive that interactions between α-SMA-positive CAFs and cholangiocarcinoma cells may be critically important to promoting ICC growth and progression, they are limited in their relevance to the *in vivo* situation by the fact that they were performed largely under 2-D culture conditions using longstanding cholangiocarcinoma cell lines of various biliary tumor cell origins, and in the case of LX-2 and LI90 cells, with long-term myofibroblastic-like cells derived from non-cholangiocarcinoma tissues. In an effort to more accurately reproduce *in vitro* the tissue architecture and complex interactive relationships between cholangiocarcinoma cells and stromal α-SMA-positive CAFs in a type I collagen matrix microenvironment reflective of desmoplastic ICC, we have now developed novel 3-dimensional (3-D) organotypic co-culture models of rat cholangiocarcinoma that closely mimic relevant histopathological, molecular, and progressive features of *in vivo* rat and human ICC. This unique *in vitro* cholangiocarcinoma model employs a 3-D gel matrix based on rat type I collagen gel to support co-culturing of a clonal strain of cholangiocarcinoma cells with a clonal α-SMA-positive CAF strain, both of which were derived from orthotopic ICC (BDEsp ICC) formed in syngeneic rat liver following bile duct inoculation of spontaneously-transformed tumorigenic rat cholangiocytes (11, 12).

Materials and Methods

Cell Lines and 3-D Organotypic Culturing

The animal experiments used to generate the orthotopic cholangiocarcinoma tumors employed in this study were performed in accordance with and approved by Virginia Commonwealth University Institutional Animal Care and Use Committee. Phenotypically distinct rat cholangiocarcinoma and desmoplastic tumor stromal-associated α-SMA-positive CAF cell lines were each obtained through selective cell harvesting and serial *in vitro* passaging (2–4 passages), using various cell enrichment conditions, of primary mixed cell outgrowths from 0.1mm tissue fragments isolated from orthotopic BDEsp ICC, as previously described (12) and as schematically depicted in Figure 1. The cholangiocarcinoma cell line was designated as BDEsp-TDE and the corresponding tumor-derived α-SMA-positive CAF cell line as BDEsp-TDF. Single cell cloning was then utilized to produce the cholangiocarcinoma (BDEsp-TDE_{H10}) and α-SMA-positive CAF (BDEsp-

TDF_{E4}) cell strains, which were used to establish the 3-D organotypic cholangiocarcinoma co-culture model described in this study. Specifically, this model was developed by co-culturing cholangiocarcinoma cells at an initial plating density of 1×10^5 cells/ml and at cell viabilities of ≥ 95% with α-SMA-positive CAFs at various initial plating densities ranging between 0-to-8 × 10^5 cells/ml (also with cell viabilities of ≥ 95%) mixed within a gel matrix of rat tail type I collagen (BD Biosciences, Bedford, MA). Cholangiocarcinoma and α-SMA-positive CAF cell strains at *in vitro* passage numbers ≤ 8 were used in the co-culture experiments. Unless otherwise specified, the cultures were maintained with our standard medium (13), for experimental periods of up to 10 days.

Gene Expression Microarray Analyses

The Affymetrix® protocol utilized for microarray analyses was previously described (12) utilizing 500ng of total RNA prepared from BDEsp ICC intact tumor samples or from cell isolates harvested at day 7 from 3-D mono- or co-cultures of BDEsp-TDE_{H10} and BDEsp-TDF_{E4} cells (serum free for 24h). As per the Affymetrix® protocol, 10μg of fragmented cRNA were hybridized on the GeneChip® Rat Expression 230 2.0 Array (Affymetrix Inc., Santa Clara, CA) for 16h at 60rpm in a 45°C hybridization oven. Every chip was scanned at a high resolution on the Affymetrix® GeneChip Scanner 3000 7G as previously described (12). Overall quality of each array was assessed by monitoring the 3′/5′ ratios for the housekeeping gene, glyceraldehyde 3-phosphate dehydrogenase (*Gapdh*), and the percentage of "Present" genes (%P). Arrays exhibiting *Gapdh* 3′/5′ < 3.0 and %P > 40% were considered good quality arrays.

Real-Time Reverse-Transcriptase Polymerase Chain Reaction (QRT-PCR)

QRT-PCR was used to validate gene expression levels of selected rat genes using TaqMan® chemistry, essentially as previously described (12). Probes and primer sets specific for the detection of rat mRNA transcripts were purchased from Applied Biosystems, Foster City, CA. These included gene-specific primer-probe sets for the following biomarker genes: *Krt19* (cytokeratin 19), ID# Rn01496870_g1; *Muc1* (mucin 1), ID# Rn01462585_m1; *Mmp7* (metalloproteinase-7, matrilysin), ID# Rn01487001_m1; *Areg* (amphiregulin), ID# Rn00567471_m1; *Acta2* (α-SMA), ID# Rn01759928_g1; *Hgf* (hepatocyte growth factor), ID# Rn00566673_m1; *Postn* (periostin), ID# Rn1494627_m1; *Sphk1* (sphingosine kinase 1), ID# Rn00682794_g1; *Cxcr4* (C-X-C chemokine receptor 4), ID# Rn01483207_m1; *Shh* (sonic hedgehog homolog), ID# Rn00568129_m1; *SMO* (Smoothened), ID# Rn00563043_m1; *Gli1* (glioblastoma 1), ID# Rn01504237_m1; *Gli2*, ID# Rn01408890_m1. *PPIA* (cyclophilin), ID# Rn00690933_m1 or *Gapdh* (glyceraldehyde 3-phosphate dehydrogenase), RefSeq: NM_017008.3 were used as controls. All QRT-PCR analyses were done in triplicate.

Histology, Immunohistochemistry, and Microscopic Imaging

Hematoxylin and eosin (H&E) staining was routinely performed on 10% formalin-fixed paraffin-embedded tissue sections of collagen gel cultures. Histochemical staining for fibrous collagen (primarily type I) was also carried out on comparably fixed and processed tissue sections from the collagen gel cultures, as well as from BDEsp-ICC using the picrosirius red staining method using reagents obtained from Polysciences, Inc. (Warrington, PA). Picrosirius red staining was viewed under a BX41 light microscope equipped with a BX-POL polarizer (Olympus Corp., Center Valley, PA). Immunohistochemical staining was performed essentially as described previously (13–15) on appropriately processed formalin-fixed, paraffin-embedded tissue sections, using the following primary antibodies: monoclonal mouse anti-human SMA (Cat. No. M0851) from DakoCytomation, Carpinteria, CA; mouse monoclonal cytokeratin 19 (CK19) (Cat. No. VP-C415) from Vector Laboratories, Burlingame, CA. Computational image analysis was used to quantify

cholangiocarcinoma spheroidal or ductal-like structures formed in 3-D mono- or co-cultures using the cellSens imaging software system (Vers. 1.4.1) from Olympus Corp. This analysis was carried out on digital images of randomized microscopic fields of 10μm thick tissue sections prepared from formalin-fixed, paraffin-embedded gel cultures stained with H&E (total number of collagen gel cultures analyzed per experimental condition: 3; total number of analyzed tissue sections per individual collagen gel culture: 2-to-4).

Invasion Assay

Cholangiocarcinoma cell migration *in vitro* (invasion) was assayed using the BD Biocoat Matrigel™ Invasion chamber (24 well plate coated with rat type 1 collagen; Matrigel-coated inserts with 8μm pore) (BD Biosciences), similar to the method described by Ohira *et al.* (16). BDEsp-TDF_{E4} cancer-associated fibroblasts were initially plated onto the collagen-coated bottom chamber of the 24 well plates at a plating density of 4×10^4 CAFs/well. Twenty-four hours later, BDEsp-TDE_{H10} cholangiocarcinoma cells were plated at 1×10^5 cells/well onto the upper surface of the Matrigel-coated insert (top chamber) of the tissue culture well. After 48 hours of incubation at 37° C (under standard culture conditions), the non-invaded cells were removed from the top surface of the Matrigel-coated porous insert with cotton-tipped swabs. The cholangiocarcinoma cells that had migrated to the lower surface of the insert were fixed with 4% paraformaldehyde and stained with 0.1% crystal violet. The migrated cells were then counted and the invasion index determined according to the manufacturer's instructions.

Statistics

For the microarray data analysis, background correction, normalization, and estimation of probe set expression summaries were performed using the log-scale robust multi-array analysis (RMA) method (17). The Student 2-tailed *t* test was used to determine *P* values, with a $P \leq 0.05$ considered significant. Statistical significance for multivariate analysis to assess probe set specific false discovery rates (FDR) was performed by estimating the *q*-values, using the Bioconductor *q-value* package (18), as previously described (12).

Results

Selective gene expression profiling of BDEsp-TDF_{E4} and BDEsp-TDE_{H10}

Gene expression profiles determined by microarray analysis for selected biomarker genes expressed in BDEsp-TDF_{E4} *versus* BDEsp-TDE_{H10} cells cultured separately or together for 7 days within rat type I collagen gel matrix are shown in Figure 2. As clearly demonstrated in Figure 2A, BDEsp-TDF_{E4} cells cultured alone in collagen gel matrix expressed a biomarker profile consistent with that of a cholangiocarcinoma-associated stromal myofibroblastic cell phenotype (4, 5), whereas BDEsp-TDE_{H10} cells cultured alone in collagen gel matrix expressed biomarker genes indicative of a neoplastic cholangiocyte origin (3, 19). Particularly noteworthy are the high levels of gene expression for extracellular matrix genes (*Postn*, collagen type 1a, fibronectin, and tenascin-C), as well as for Mmp2 and 11, insulin-like growth factor binding proteins 5 and 7, platelet derived growth factor receptor-β, vimentin, WNT1 inducible signaling protein 1, and desmin selectively exhibited by the cultured BDEsp-TDF_{E4} cells. In *contrast*, BDEsp-TDE_{H10} cells cultured alone under identical conditions were characterized by their high levels of gene expression for biliary cell *Krt 7* and *19*, E-cadherin, *Muc1*, and *Areg*. The gene expression pattern for specific integrins was also determined to be distinctly different for BDEsp-TDF_{E4} *versus* BDEsp-TDE_{H10} in monoculture in type I collagen gel matrix, with integrin β_5 (*Itg*β_5) mRNA being predominantly expressed in the CAFs and *Itg*β_4 mRNA being most highly expressed in the cholangiocarcinoma cells (Supplemental Figure 1). In addition, our QRT-PCR analyses confirmed cultured BDEsp-TDE_{H10} cellsto selectively express mRNA

for *Krt19*, *Muc1*, *Mmp-7*, and *Areg*, when compared against cultured BDEsp-TDF$_{E4}$ cells, and conversely, cultured BDEsp-TDF$_{E4}$ cells differentially expressed mRNA for *Acta2* (α-SMA), *Hgf, Postn,* and *Sphk1* (Supplemental Figure 2). Gene members of the Hedgehog (Hh) signaling pathway were also demonstrated by QRT-PCR to be differentially expressed in the BDEsp-TDE$_{H10}$ *versus* BDEsp-TDF$_{E4}$ cultures, with *Shh* being largely expressed in the cholangiocarcinoma cell strain and *SMO*, *Gli1* and *Gli2* being predominantly expressed in the CAF strain (Supplemental Figure 3).

Organotypic 3-D co-culture of BDEsp-TDF$_{E4}$ and BDEsp-TDE$_{H10}$ cells in type I collagen gel matrix closely mimics desmoplastic BDEsp ICC

As depicted in Figure 3, 3-D organotypic co-cultures of CK19 (Krt 19)-positive BDEsp-TDE$_{H10}$ cholangiocarcinoma cells and α-SMA-positive BDEsp-TDF$_{E4}$ CAFs in rat type I collagen gel matrix reproduce characteristic histopathological features of desmoplastic BDEsp ICC *in vivo*, including enhanced histochemical staining for type I collagen secreted into the matrix (Figure 3E). Furthermore, our microarray data shown in Figure 2B revealed the organotypic α-SMA-positive CAF/cholangiocarcinoma co-cultures to exhibit an RMA expression summary for CAF and cholangiocarcinoma biomarker genes closely paralleling that of resected whole BDEsp ICC tumor tissue.

BDEsp-TDF$_{E4}$ CAFs promote BDEsp-TDE$_{H10}$ cholangiocarcinoma cell growth and invasion in co-culture

BDEsp-TDE cholangiocarcinoma cells when cultured alone in rat type 1 collagen gel matrix form into 3-D spheroid structures, which when viewed in routine H & E stained histological sections appear in cross-section as duct-like structures mimicking in their morphology the neoplastic ducts of well differentiated BDEsp ICC from which they were derived (Figure 4). As further demonstrated in Figure 5B *versus* 5A, and histological sections shown in Figure 6A-D, co-culturing BDEsp-TDE$_{H10}$ with BDEsp-TDF$_{E4}$ cells under our 3-D organotypic culture conditions profoundly increased the number of cholangiocarcinoma cell spheroid/duct-like structures formed in the collagen gel matrix over those formed in the absence of BDEsp-TDF$_{E4}$ cells. Furthermore, as demonstrated in Figure 6D, the mean number of spheroid/duct-like structures formed per cm^2 section area in randomly analyzed histological preparations of the gel cultures significantly increased as a function of higher initial BDEsp-TDF$_{E4}$ cell plating densities when the ICC-derived cancer cells and CAFs were co-cultured for 6 days in rat type I collagen gel matrix, correlating with an increasing shrinkage of the collagen gel substratum. A more progressive cholangiocarcinoma cell phenotype also resulted from organotypic co-culturing of the BDEsp-TDF$_{E4}$ cells with BDEsp-TDE$_{H10}$ cells compared to mono-cultures of cholangiocarcinoma cells only (Figure 6B & C *versus* 6A). Moreover, BDEsp-TDE$_{H10}$ cholangiocarcinoma cells exhibited significantly increased *in vitro* invasiveness when assayed in the presence *versus* absence of BDEsp-TDF$_{E4}$ CAFsusing the Matrigel invasion chamber.

Interaction between BDEsp-TDF$_{E4}$ and BDEsp-TDE$_{H10}$ cells induces up-regulation of genes linked to cholangiocarcinoma progression and/or invasion

Both Muc1 and CXCR4 have been suggested to play key roles in promoting ICC progression and/or migration/invasion (3, 5, 19, 20). Here it is relevant that culturing BDEsp-TDE$_{H10}$ cholangiocarcinoma cells in the presence of BDEsp-TDF$_{E4}$ CAFs or conditioned medium from BDEsp-TDF$_{E4}$ cultures significantly increased both *Cxcr4* and *Muc1* expression in the cholangiocarcinoma cells (Figure 7). In comparison, conditioned medium from BDEsp-TDE$_{H10}$ cultures produced a significant up-regulation of *Hgf* expression in cultured BDEsp-TDF$_{E4}$ cells (Figure 7B). The data shown in Figure 7C & D further suggest that HGF produced by BDEsp-TDF$_{E4}$ CAFs is the likely inducer of increased *Cxcr4* gene expression in the cholangiocarcinoma cells. Recombinant HGF has

also been recently reported to up-regulate *Cxcr4* expression in cultured human glioma cells (21). In contrast, *Muc1* up-regulation in cultured BDEsp-TDE_{H10} cells was determined by us not to be up-regulated by HGF (data not shown).

Discussion

Organotypic culture models have been developed for different tumor types, including breast, prostate, pancreatic, ovarian, and esophageal cancers (22–25). However, to our knowledge, there have been no previous reports describing the development of a 3-D culture model based on co-culturing of α-SMA-positive CAFs and cholangiocarcinoma cells simultaneously derived from orthotopic ICC.

Unique features distinguishing this novel 3-D co-culture model include: (1) its construction using "phenotypically pure" α-SMA-positive CAF and cholangiocarcinoma cell strains derived from desmoplastic ICC formed from spontaneously transformed rat cholangiocytes orthotopically transplanted into syngeneic rat liver; (2) α-SMA-positive CAFs and cholangiocarcinoma cells used to establish this organotypic rat cholangiocarcinoma model each exhibited characteristic gene expression profiles for select classes of genes (e.g., matricellular proteins, growth factor/chemokines and receptors, mucins, proteases, integrins, Hh family members) relevant to cholangiocarcinogenesis; (3) the identification of gene expression profiles using this novel 3-D cellular model closely resembled that of tissue samples obtained from parental BDEsp cholangiocarcinoma grown orthotopically; (4) 3-D co-culturing of rat cholangiocarcinoma cells and α-SMA-positive CAFs derived from the same rat ICC type significantly enhanced "duct-like" growth and cancer cell migration/invasion, as well as augmented type I collagen deposition into the gel matrix so as to mimic *in vitro* the desmoplastic stroma of the parental tumor; (5) α-SMA-positive CAF-cholangiocarcinoma cell interactions resulted in up-regulated gene expression of *Hgf, Cxcr4, and Muc1,* each of which has been associated with cholangiocarcinoma cell invasiveness and/or poorer survival outcomes for ICC patients following tumor resection (3–5, 16, 20, 26); and (6) HGF produced by α-SMA-positive CAFs is an inducer of significant *Cxcr4* overexpression in cholangiocarcinoma cells.

Our histological data further indicate that 3-D co-culturing of rat cholangiocarcinoma cells with α-SMA-positive CAFs within a type I collagen gel matrix closely reproduces characteristic morphological features of the parental orthotopic BDEsp tumor, also resembling the histopathology of well-differentiated, desmoplastic tubular ICC in humans. Moreover, this organotypic rat cholangiocarcinoma model was found to exhibit gene expression profiles reflecting highly expressed CAF (e.g., *Postn*, *Tnc*) and cholangiocarcinoma genes (e.g., *Muc1*), whose overexpression in human ICC has been reported to be significantly correlated with human ICC progression, as well as shorter patient survival times following surgical resection (3, 5, 20, 27).

Overexpression of *Postn* in cholangiocarcinoma-derived myofibroblastic cells and of *Muc1* in cholangiocarcinoma cells have also been observed by us to correlate with increased malignancy in our orthotopic ICC syngeneic rat model (11, 12). In addition, we have now determined that BDEsp transformants stably transfected to overexpress rat *Postn* or *Muc1* cDNA exhibit significantly enhanced cell migration/invasion *in vitro* compared with that of corresponding empty vector and untransfected BDEsp controls (Sirica, A. E., *et al.*, unpublished data). Although these latter findings are preliminary, they suggest a molecular strategy for ICC therapy based on combinational targeting of *Postn* and *Muc1* as candidate gene pathways related to ICC invasive growth. Such a novel molecular therapeutic strategy can now be readily tested in the complementary organotypic culture and orthotopic cholangiocarcinoma syngeneic rat models that are currently available in our laboratory.

The 3-D organotypic culture model of cholangiocarcinoma described in his study appears to be very well suited to serve as a pathophysiologically relevant *in vitro* system to investigate key stromal/cancer cell interactions mediated by aberrantly expressed CAF or cholangiocarcinoma genes postulated to accelerate ICC malignancy (3– 5). It is also anticipated that this 3-D culture model, combined with its complementary parent orthotopic ICC, syngeneic rat model (11), will also prove to be invaluable as preclinical platforms for rapidly assessing mechanism-based therapeutic strategies targeting interactive pathways correlated with ICC progression. Future studies are now needed to validate these complementary *in vitro* and *in vivo* syngeneic models for use in identifying and testing molecular targeting strategies for ICC therapy. Moreover, our current study also suggests the feasibility of establishing an organotypic model of human desmoplastic cholangiocarcinoma potentially suitable for screening therapeutic agents that would be similarly based on 3-D culturing within type I collagen matrix of cholangiocarcinoma and α-SMA-positive CAF cell lines/stains simultaneously established from primary cell isolates derived from surgically resected human ICC tissues. In this context, establishment of primary cultures of α-SMA-positive CAF from human ICCs has been described (7, 27), and methods to generate cholangiocarcinoma cell lines from resected human ICC tissues are now well established. Thus, 3-D organotypic modeling of human desmoplastic ICC now seems plausible and should be pursued.

Supplementary Material

Refer to Web version on PubMed Central for supplementary material.

Acknowledgments

Grant Support: Supported by NIH grants R01 CA 039225 and R01 CA 083650 (A.E.S.)

References

1. Terada T, Makimoto K, Terayama N, et al. Alpha-smooth muscle actin-positive stromal cells in cholangiocarcinomas, hepatocellular carcinomas and metastatic liver carcinomas. J Hepatol. 1996; 24:706–712. [PubMed: 8835746]
2. Okamura N, Yoshida M, Shibuya A, et al. Cellular and stromal characteristics in the scirrhous hepatocellular carcinoma: comparison with hepatocellular carcinomas and intrahepatic cholangiocarcinomas. Pathol Int. 2005; 55:724–731. [PubMed: 16271085]
3. Sirica AE, Dumur CI, Campbell DJ, et al. Intrahepatic cholangiocarcinoma progression: prognostic factors and basic mechanisms. Clin Gastroenterol Hepatol. 2009; 7:S68–S78. [PubMed: 19896103]
4. Sirica AE, Campbell DJ, Dumur CI. Cancer-associated fibroblasts in intrahepatic cholangiocarcinoma. Curr Opin Gastroenterol. 2011; 27:276–284. [PubMed: 21297470]
5. Sirica AE. The role of cancer-associated myofibroblasts in intrahepatic cholangiocarcinoma. Nat Rev Gastroenterol Hepatol. 2012; 9:44–54. [PubMed: 22143274]
6. Okabe H, Beppu T, Hayashi H, et al. Hepatic stellate cells may relate to progression of intrahepatic cholangiocarcinoma. Ann Surg Oncol. 2009; 16:2555–2564. [PubMed: 19548033]
7. Chuaysri C, Thuwajit P, Paupairoj A, et al. Alpha-smooth muscle actin-positive fibroblasts promote biliary cell proliferation and correlate with poor survival in cholangiocarcinoma. Oncol Rep. 2009; 21:957–969. [PubMed: 19287994]
8. Murakami K, Abe T, Miyazawa M, et al. Establishment of a new human cell line, LI90, exhibiting characteristics of hepatic Ito (fat-storing) cells. Lab Invest. 1995; 72:731–739. [PubMed: 7540235]
9. Xu L, Hui AY, Albanis E, et al. Human hepatic stellate cell lines, LX-1 and LX-2: new tools for analysis of hepatic fibrosis. Gut. 2005; 54:142–151. [PubMed: 15591520]
10. Okabe H, Beppu T, Hayashi H, et al. Hepatic stellate cells accelerate the malignant behavior of cholangiocarcinoma cells. Ann Sur Oncol. 2011; 18:1175–1184.

11. Sirica AE, Zhang Z, Lai GH, et al. A novel “patient-like” model of cholangiocarcinoma progression based on bile duct inoculation of tumorigenic rat cholangiocyte cell lines. Hepatology. 2008; 47:1178–1190. [PubMed: 18081149]
12. Dumur CI, Campbell DJ, DeWitt JL, et al. Differential gene expression profiling of cultured *neu*-transformed *versus* spontaneously-transformed rat cholangiocytes and of corresponding cholangiocarcinomas. Exp Mol Pathol. 2010; 89:227–235. [PubMed: 20816680]
13. Lai GH, Zhang Z, Shen XN, et al. *erbB-2/neu* transformed rat cholangiocytes recapitulate key cellular and molecular features of human bile duct cancer. Gastroenterology. 2005; 129:2047–2057. [PubMed: 16344070]
14. Sirica AE, Gainey TW. A new rat bile ductular epithelial cell culture model characterized by the appearance of polarized bile ducts in vitro. Hepatology. 1997; 26:537–549. [PubMed: 9303480]
15. Lai GH, Radaeva S, Nakamura T, et al. Unique epithelial cell production of hepatocyte growth factor/scatter factor by putative precancerous intestinal metaplasias and associated “intestinal-type” biliary cancer chemically induced in rat liver. Hepatology. 2000; 31:1257–1265. [PubMed: 10827151]
16. Ohira S, Sasaki M, Harada K, et al. Possible regulation of migration of intrahepatic cholangiocarcinoma cells by interactions of CXCR4 expressed in carcinoma cells with tumor necrosis factor-α and stromal-derived factor-1 released in stroma. Am J Pathol. 2006; 168:1155–1168. [PubMed: 16565491]
17. Irizarry RA, Bolstad BM, Collin F, et al. Summaries of Affymetrix GeneChip probe level data. Nucleic Acids Res. 2003; 31:e15. [PubMed: 12582260]
18. Storey JD. A direct approach to false discovery rates. JR Stat Soc B. 2002; 64:479–498.
19. Sirica AE, Nathanson MH, Gores GJ, et al. Pathobiology of biliary epithelia and cholangiocarcinoma: proceedings of the Henry M. and Lillian Stratton Basic Research Single-Topic Conference. Hepatology. 2008; 48:2040–2046. [PubMed: 18855901]
20. Park SY, Roh SJ, Kim YN, et al. Expression of MUC1, MUC2, MUC5AC and MUC6 in cholangiocarcinoma: prognostic impact. Oncology Reports. 2009; 22:649–657. [PubMed: 19639217]
21. Esencay M, Newcomb EW, Zagzag D. HGF upregulates CXCR4 expression in gliomas via NF-κB: implications for glioma cell migration. J Neurooncol. 2010; 99:33–40. [PubMed: 20157762]
22. Chioni A-M, Grose R. Organotypic modelling as a means of investigating epithelial-stromal interatcions during tumourigenesis. Fibrogenesis Tissue Repair. 2008; 1:8. [PubMed: 19077226]
23. Froeling FEM, Mirza TA, Feakins RM, et al. Organotypic culture model of pancreatic cancer demonstrates that stromal cells modulate E-cadherin, β-catenin, and Ezrin expression in tumor cells. Am J Pathol. 2009; 175:636–648. [PubMed: 19608876]
24. Froeling FEM, Marshall JF, Kocher HM. Pancreatic cancer organotypic cultures. J Biotechnol. 2010; 148:16–23. [PubMed: 20083148]
25. De Wever O, Hendrix A, De Boeck A, et al. Modeling and quantification of cancer cell invasion through collagen type I matrices. Int J Dev Biol. 2010; 54:887–896. [PubMed: 19757378]
26. Matsumoto K, Nakamura T. Hepatocyte growth factor and the met system as a mediator of tumor-stromal interactions. Int J Cancer. 2006; 119:477–483. [PubMed: 16453287]
27. Utispan K, Thuwajit P, Abiko Y, et al. Gene expression profiling of cholangiocarcinoma-derived fibroblasts reveals alterations related to tumor progression and indicates periostin as a poor prognostic marker. Mol Cancer. 2010; 9:13. [PubMed: 20096135]

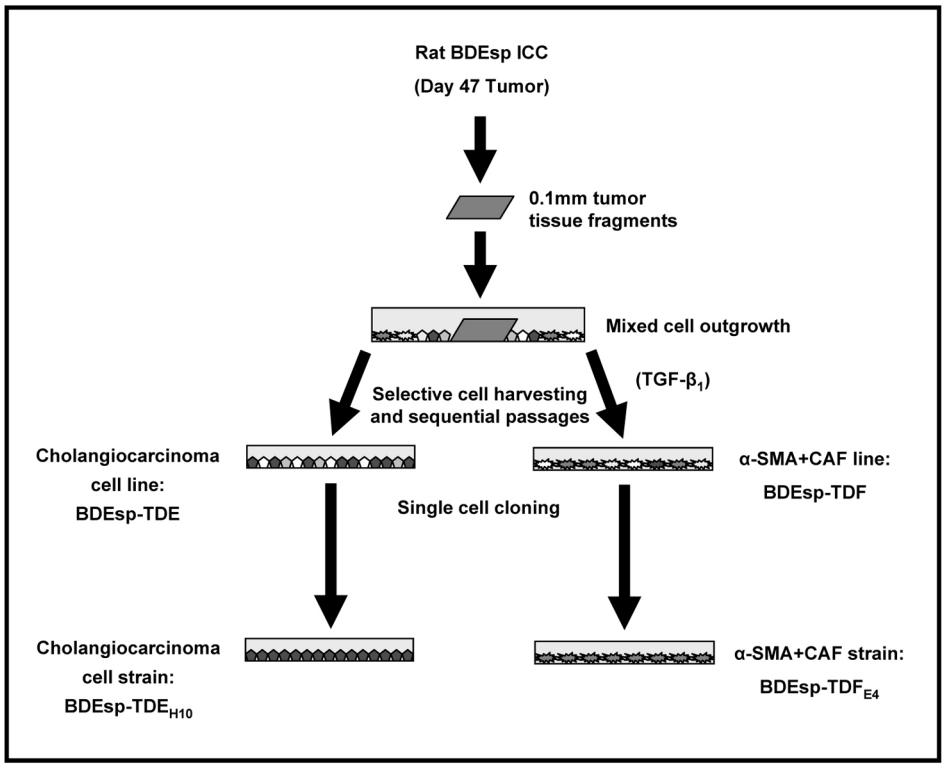

Figure 1.

Scheme outlining the method used to concomitantly establish the BDEsp-TDE_{H10} cholangiocarcinoma celland BDEsp-TDF_{E4} cancer-associated fibroblastic (CAF) cellstrains derived from an orthotopic BDEsp ICC obtained from syngeneic rat liver at day 47 after bile duct inoculation of the tumorigenic, spontaneously-transformed rat cholangiocyte cell line (BDEsp). As an initial selection step, TGF-β1 at 5ng/ml was temporarily added to the culture medium to facilitate expansion of the CAF population.

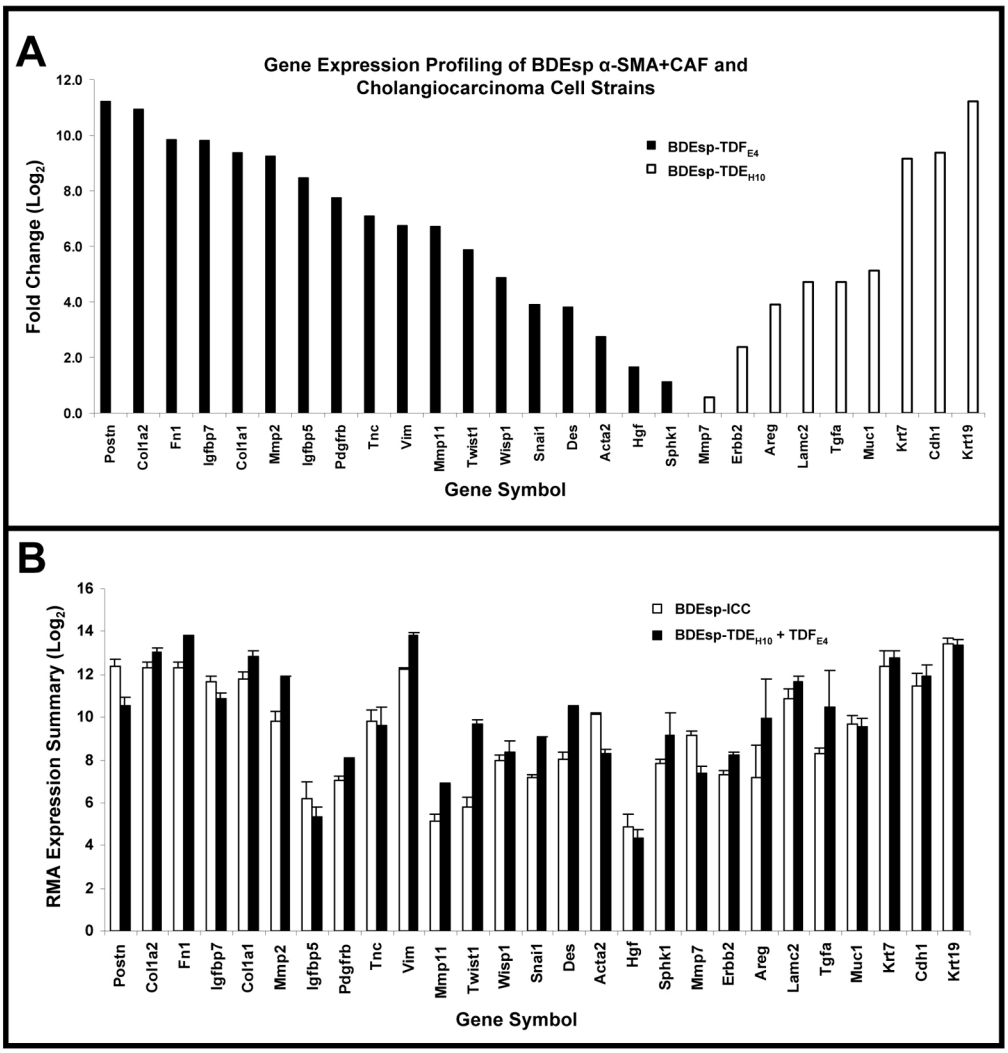

Figure 2.

Gene expression profiling based on selected gene biomarkers of BDEsp ICC-derived cancer-associated myofibroblastic cells and cholangiocarcinoma cell strains. (**A**) Bar chart representation of 27 marker genes assessed by microarray analysis that showed significant differences in expression levels between BDEsp-TDF_{E4} and BDEsp-TDE_{H10} when cultured individually in a rat tail type I collagen gel matrix. (**B**) Robust Multiarray Analysis (RMA) expression summaries for the 27 analyzed biomarker genes shown in A, comparing orthotopic BDEsp ICC to organotypic BDEsp-TDF_{E4}/BDEsp-TDE_{H10} culture. *Postn*, periostin; *Col1a2*, collagen type Ia2; *Fn1*, fibronectin 1; *Igfbp7,* insulin-like growth factor binding protein 7; *Col1a1*, collagen type Ia1; *Mmp2*, metalloproteinase-2; *Igfbp5*, insulin-like growth factor binding protein 5; *Pdgfrb*, platelet-derived growth factor receptor β; *Tnc*, tenascin-C; *Vim*, vimentin; *Mmp11*, metalloproteinase 11; *Twist1*, Twist homolog 1; *Wisp1*, WNT1 inducible signaling protein 1; *Snail1*, Snail homolog 1; *Des*, desmin; *Acta2*, smooth muscle actin; *Hgf*, hepatocyte growth factor; *Sphk1*, sphingosine kinase 1; *Mmp7*, metalloproteinase-7; *Erbb2*, c-erbB2 protooncogene receptor protein; *Areg*, amphiregulin; *Lamc2*, laminin gamma2; *Tgfa*, transforming growth factor α; *Muc1*, mucin 1; *Krt7*, cytokeratin 7; *Cdh1*, E-cadherin; *Krt19*, cytokeratin 19.

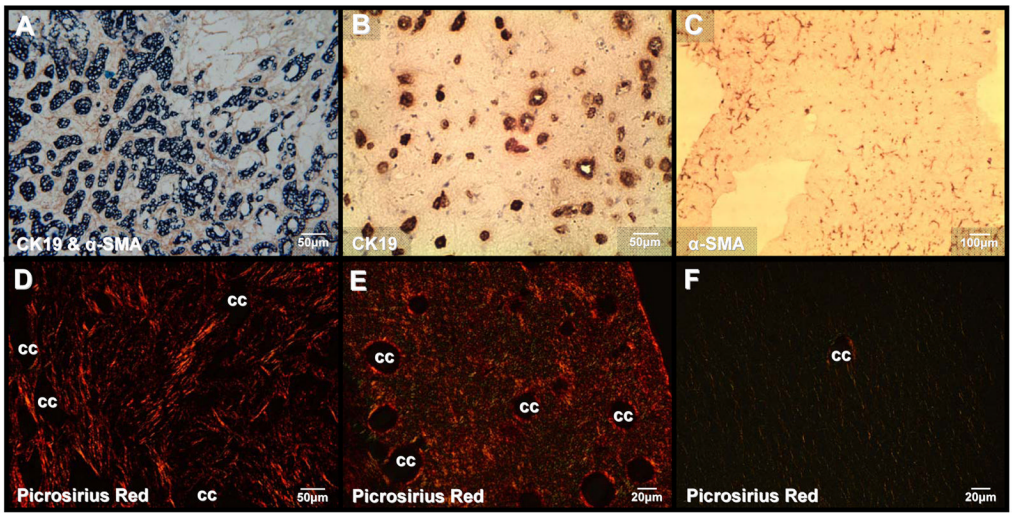

Figure 3.

Co-culturing of BDEsp-TDE$_{H10}$ cells with BDEsp-TDF$_{E4}$ cells in rat tail type I collagen gel matrix reproduces characteristic histopathological features of desmoplastic BDEsp ICC *in vivo*. (**A**) Desmoplastic BDEsp ICC formed in rat liver showing selective positive immunostaining of well differentiated cholangiocarcinoma ducts for biliary cytokeratin 19 (CK19) (blue staining) and cancer-associated myofibroblastic cells positive for α-smooth muscle actin (α-SMA) (brown staining) in the surrounding tumor stroma. (**B**) Like BDEsp ICC, well differentiated "duct-like" structures formed from BDEsp-TDE$_{H10}$ cells in organotypic co-culture exhibit selective immunoreactivity for CK19 (brown staining). (**C**) Also like BDEsp ICC, stromal BDEsp-TDF$_{E4}$ cells in organotypic co-culture are selectively immunoreactive for α-SMA (brown staining). (**D**) Picrosirius red staining under polarized light of type I collagenous fibers (orange-yellow) densely populating the desmoplastic stroma of a BDEsp ICC. (**E**) Picrosirius red staining of a representative histological section of a BDEsp-TDE/BDEsp-TDF co-culture mimicking the strong extracellular staining reaction for type I collagen exhibited by the orthotopic ICC in **D**. (**F**) Picrosirius red staining of a BDEsp-TDE$_{H10}$ control culture without BDEsp-TDF showing only background staining for type I collagen fibers in gel matrix. cc denotes representative cholangiocarcinoma ducts or "duct-like" structures.

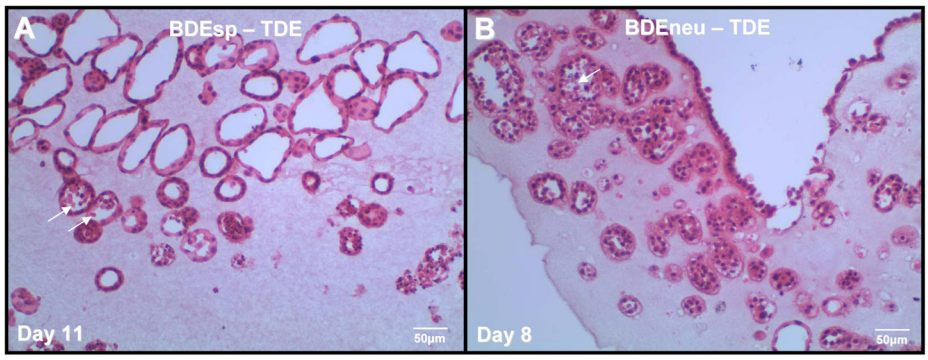

Figure 4.

Representative H & E stained histological section of our rat cholangiocarcinoma cell line BDEsp-TDE at *in vitro* passage 3, derived from well differentiated BDEsp ICC, and cultured alone for 11 days within rat tail type I collagen gel matrix. Note that the cholangiocarcinoma cells are organized into well differentiated "duct-like" structures reminiscent of those observed in histological sections of the parent low grade BDE ICC. For comparison, the photomicrograph in (**B**) demonstrates a rat cholangiocarcinoma cell line designated as BDEneu-TDE that was established in our laboratory from a more highly malignant and moderately-differentiated ICC formed in syngeneic rat liver after bile duct inoculation of oncogenic-*neu* transformed rat cholangiocytes. As demonstrated in **B**, rat BDEneu-TDE cells in organotypic culture in a type I collagen gel matrix reflect the less differentiated "duct-Like" phenotype of the parent orthotopic tumor. In both **A** & **B**, arrows point to dead cells within the lumens of some of the neoplastic "duct-like" structures, indicating that cells within the central areas of formed cholangiocarcinoma cell spheroids are likely undergoing apoptotic cell death.

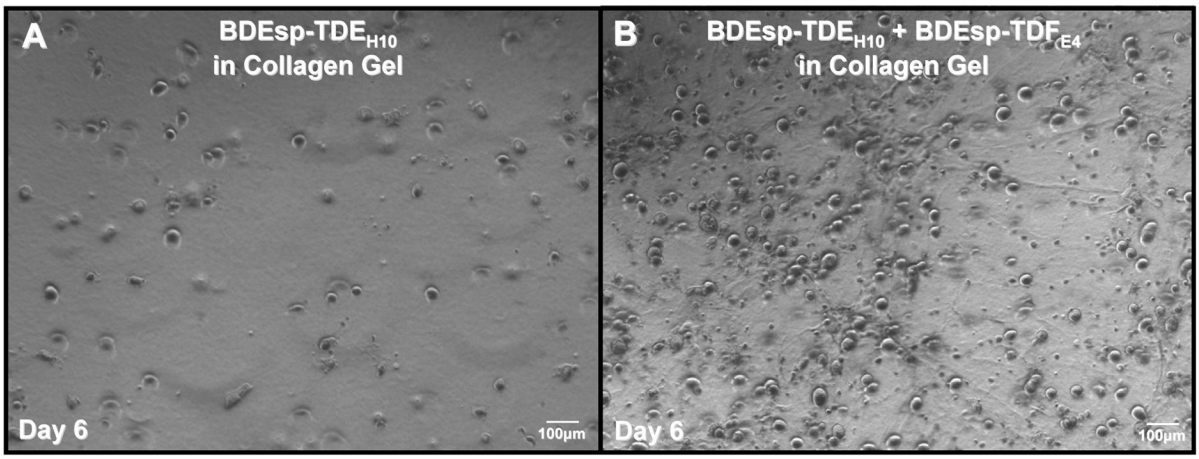

Figure 5.

Representative phase contrast photomicrographs of (**A**) rat BDEsp-TDE$_{H10}$ cholangiocarcinoma cells cultured alone for 6 days in rat tail type I collagen gel compared with (**B**) in which the BDEsp-TDE$_{H10}$ cells were co-cultured under comparable conditions over the same time period with BDEsp-TDF$_{E4}$ CAFs. Compare with the photomicrographs of the H & E stained histological sections shown in Figure 6, noting the marked increase in 3-dimensional cell spheroids formed in the co-culture over those observed in the cholangiocarcinoma cell monoculture.

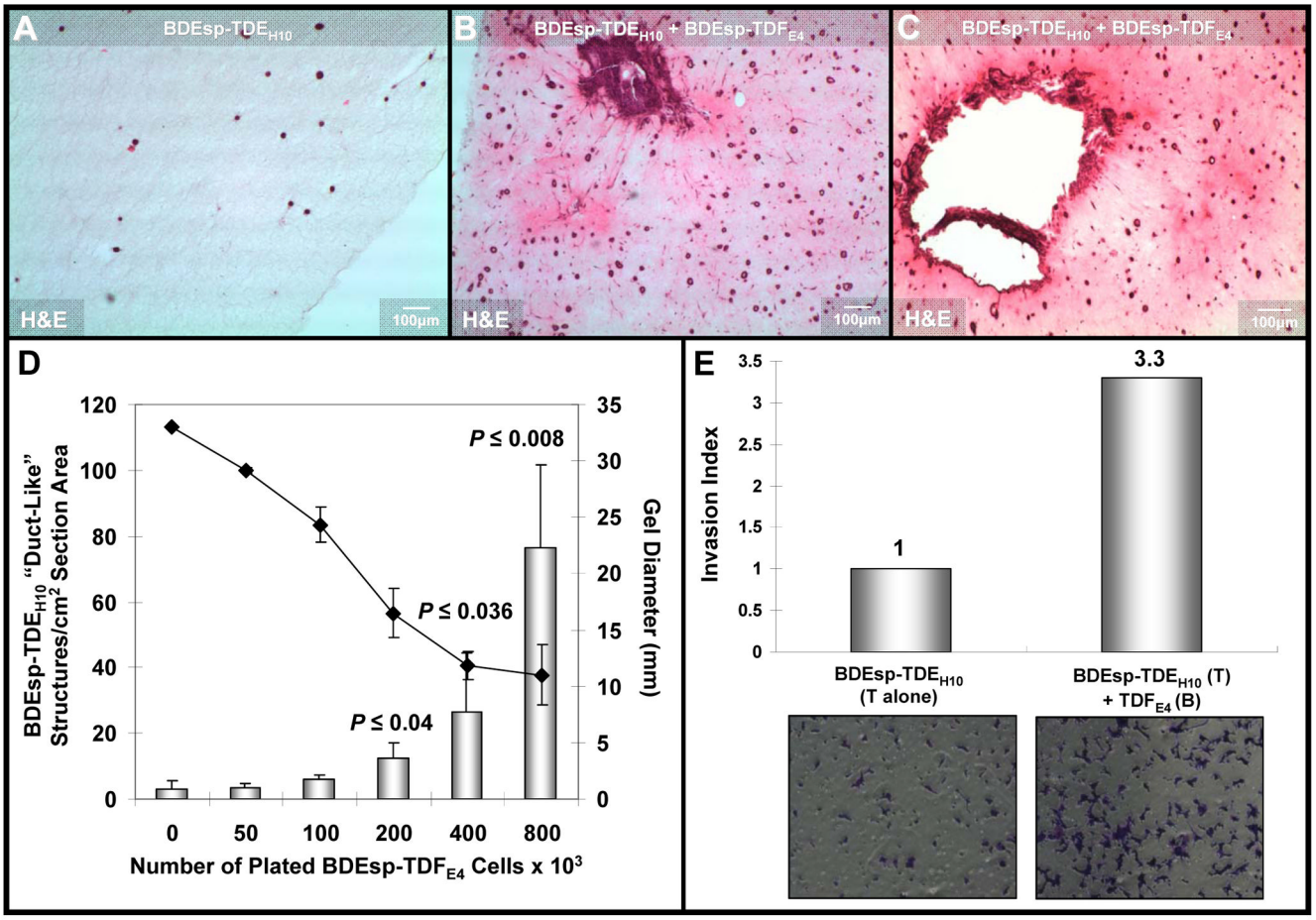

Figure 6.

Photomicrographs of representative H & E stained histological sections of 3-dimensional organotypic cultures of BDEsp-TDE$_{H10}$ cholangiocarcinomacells cultured for 6 days either in monoculture (**A**) or in co-culture with BDEsp-TDF$_{E4}$ CAFs (**B** & **C**). Cholangiocarcinoma cells were initially plated at a cell density of 2×10^5 cells/type I collagen gel in both the mono- and co-cultures. The initial CAF cell plating density in the co-cultures was at 8×10^5 cells/gel. The histological section shown in B was obtained in the same experiment as that for **A**, whereas that in **C** was from a separate experiment essentially repeating the culture conditions used for **B**. Note the dramatic increase in the number of spheroidal/"duct-like" structures formed from the cholangiocarcinoma cells in the co-cultures (**B** & **C**) over those formed under comparable culture conditions in control cholangiocarcinoma cell monoculture without CAFs (A). Also observe a much more intense eosinophilic staining of the gel matrix in **B** & **C** compared to that of **A**, indicative of an increase in the cellular secretion of insoluble proteins into the co-culture matrix *versus* that produced in the cholangiocarcinoma cell monoculture. As further depicted in **B** & **C**, only the co-cultures exhibited prominent irregular clusters of anaplastic cholangiocarcinoma cells surrounded by stromal CAFs, reflective of malignant progression and apparent invasiveness. (**D**) Bar graph demonstrating the mean number of spheroidal/"duct-like" structures/cm^2 tissue section area formed from BDEsp-TDE$_{H10}$ cholangiocarcinoma cells to significantly increase as a function of higher initial BDEsp-TDF$_{E4}$ plating densities when these ICC derived cell types were co-cultured for 6 days in rat type I collagen gel matrix. Each value represents the mean ± SD determined from microimaging measurements made on 10μm

thick H & E stained histological sections (n = at least 2 sections/slide prepared from triplicate cultures for each CAF plating density). *P* values were determined against the 0 CAF culture condition. Gel contraction, measured as a reduction in mm gel diameter (= mean ± SD) was determined to be significantly greater at the higher initial BDEsp-TDF_{E4} cell plating densities. (**E**) Representative data demonstrating BDEsp-TDF_{E4} CAFsto increase the cell migration/invasiveness of BDEsp-TDE_{H10} cholangiocarcinoma cells *in vitro* when assessed in the Matrigel™ invasion bioassay system. T= top chamber coated by Matrigel; B = bottom culture well coated with rat tail type I collagen. Invasion Index was determined according to the manufacturer's instructions.

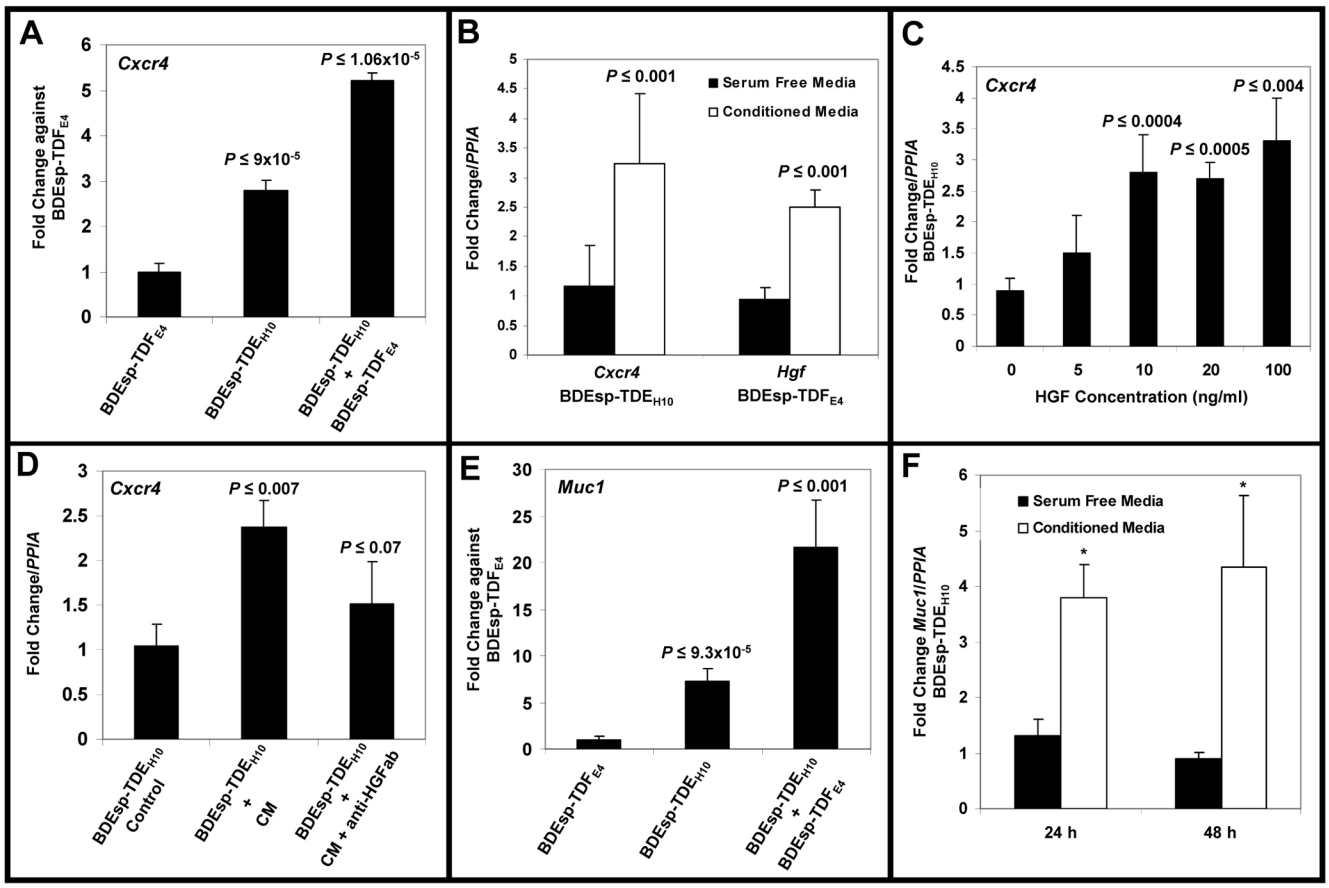

Figure 7.

(**A**) TaqMan® QRT-PCR data demonstrating that co-culturing of rat BDEsp-TDE$_{H10}$ cholangiocarcinoma cells in rat tail type I collagen gel matrix in the presence of BDEsp-TDF$_{E4}$ CAFs grown to confluence on type I collagen-coated plastic significantly induced *Cxcr4* gene expression in the cholangiocarcinoma cells over monoculture cell values. (**B**). QRT-PCR data showing conditioned medium from cultured BDEsp-TDF$_{E4}$ cells to significantly up-regulate *Cxcr4* gene expression in BDEsp-TDE$_{H10}$ cholangiocarcinoma cells cultured alone on type I collagen-coated plastic, whereas conditioned medium from BDEsp-TDE $_{H10}$ cells significantly induced Hgf gene expression in BDEsp-TDF$_{E4}$ cells cultured alone under identical conditions. (**C**) QRT-PCR data showing a significant concentration-dependent increase in *Cxcr4* gene expression in cultured BDEsp-TDE$_{H10}$ cells following exposure over a 48-hour treatment period to recombinant human HGF. (**D**) QRT-PCR data showing the effect of conditioned medium from cultured BDEsp-TDF$_{E4}$ CAFs on up-regulating *Cxcr4* gene expression in cultured BDEsp-TDE$_{H10}$ cholangiocarcinoma cells is partially blocked by the addition of neutralizing HGF antibody (anti-HGFab). (**E**) QRT-PCR data demonstrating that co-culturing of BDEsp-TDE$_{H10}$ cholangiocarcinoma cells in the presence of BDEsp-TDF$_{E4}$ CAFs under identical conditions as in **A** also produced a significant up-regulation of *Muc1* gene expression in the cholangiocarcinoma cells over monoculture cell values. (**F**) Similar to **B**, conditioned medium from cultured BDEsp-TDF$_{E4}$ CAFs induced a significant increase in *Muc1* gene expression in cultured BDEsp-TDE$_{H10}$ cholangiocarcinoma cells. *PPIA* (cyclophilin A) was used as the housekeeping gene to normalize *Cxcr4, Hgf* and *Muc1* gene expression. Comparable QRT-PCR results were also obtained when normalized with *Gapdh*. Each value

represents the mean ± SD, obtained from determinations made on a minimum of six cultures per experimental condition.